N-acetylcysteine induces apoptosis via the mitochondria-dependent pathway but not via endoplasmic reticulum stress in H9c2 cells

YUYONG LIU[1*], KE LIU[2,3*], NIAN WANG[2,3] and HUALI ZHANG[2,3]

[1]Beijing Institute of Heart, Lung and Blood Vessel Disease, Capital Medical University Affiliated to Beijing Anzhen Hospital, Beijing 100029; [2]Department of Pathophysiology and [3]Hunan Province Key Laboratory of Sepsis Translational Medicine, Xiangya School of Medicine, Central South University, Changsha, Hunan 410078, P.R. China

Received August 1, 2016; Accepted July 18, 2017

DOI: 10.3892/mmr.2017.7442

Abstract. *N*-acetylcysteine (NAC), a precursor of glutathione, is a widely used thiol-containing antioxidant and modulator of the intracellular redox state. Our previous study demonstrated that excess reduced glutathione (GSH) from NAC treatment paradoxically led to a reduction in glutathione redox potential, increased mitochondrial oxidation and caused cytotoxicity at lower reactive oxygen species levels in H9c2 cells. However, no detailed data are available on the molecular mechanisms of NAC-induced cytotoxicity on H9c2 cells. In the present study, it was demonstrated that NAC-induced cytotoxicity towards H9c2 cells was associated with apoptosis. The activation of caspase-9 and -3, and cleavage of procaspase-9 and -3, but not of caspase-8, were involved in NAC-induced apoptosis. The dissipation of mitochondrial transmembrane potential, release of cytochrome *c*, translocation of B cell lymphoma-2 (Bcl-2)-associated X protein (Bax) to the mitochondria, and the increased ratio of Bax/Bcl-2 mRNA indicated that NAC treatment-induced apoptosis occurred mainly through the mitochondria-dependent pathway. Redox western blot analysis demonstrated that NAC did not disrupt the highly oxidized environment of the endoplasmic reticulum, which was indicated by maintenance of the oxidized form of protein disulfide isomerase, an essential chaperone in the formation of disulfide bond formation in the endoplasmic reticulum. In addition, no significant changes in the expression of binding immunoglobulin protein or C/EBP homologous protein were apparent in the process of NAC-induced apoptosis. Taken together, the present study demonstrated for the first time, to the best of our knowledge, that NAC induced apoptosis via the mitochondria-dependent pathway but not via endoplasmic reticulum stress in H9c2 cells, and the exogenous GSH from NAC did not alter the oxidized milieu of the endoplasmic reticulum.

Correspondence to: Dr Nian Wang or Dr Huali Zhang, Department of Pathophysiology, Xiangya School of Medicine, Central South University, 110 Xiangya Road, Changsha, Hunan 410078, P.R. China
E-mail: csuwangnian@163.com
E-mail: zhanghuali@csu.edu.cn

*Contributed equally

Key words: *N*-acetylcysteine, apoptosis, mitochondria-dependent pathway, endoplasmic reticulum

Introduction

Redox homeostasis is essential for normal intracellular metabolism (1). It is well established that oxidative stress is critical in the pathophysiology of several diseases (2). Reductive stress is the counterpart of oxidative stress, and is defined as an abnormal increase of reducing equivalents (3). An increasing number of studies have focused on the deleterious effects of reductive stress in unicellular eukaryotic and mammalian cells (4,5). Potent, exogenous reductants, including dithiothreitol (DTT), are widely used to disrupt disulfide bond formation and abrogate oxidative protein folding in the endoplasmic reticulum (ER), which triggers reductive stress and the ER stress response (6). Previous findings describing experimental mice found associations with the dysregulation of glutathione homeostasis and protein aggregation cardiomyopathy (5). However, despite decades of studies on redox biology, the molecular and cellular mechanisms underlying reductive stress remain to be fully elucidated.

Maintenance of the glutathione redox couple, reduced glutathione (GSH)/oxidized glutathione (GSSG), is achieved by recycling via the pentose phosphate pathway and GSH biosynthesis. *N*-acetylcysteine (NAC), a precursor of GSH, is a widely used thiol-containing antioxidant and modulator of the intracellular redox state. NAC has attracted interest for its antioxidant property, and increasing evidence has demonstrated that repletion of the levels of GSH through NAC can protect against oxidative stress-induced cell death though scavenging free radicals (7,8).

Previous studies have demonstrated that NAC can induce apoptosis in vascular smooth muscle cells, enhance fisetin-induced apoptosis in colorectal carcinoma cell lines, and induce hypoxia-induced apoptosis in murine embryonic

fibroblasts (9-11). Our previous study demonstrated that excess GSH from NAC treatment in H9c2 cells caused a further reduction of glutathione redox potential (GSSG/2GSH), increased mitochondrial oxidation and caused cytotoxicity in the presence of lower reactive oxygen species (ROS) levels (12). However, the molecular mechanisms have not been investigated. In the present study, the mechanisms of NAC-induced cytotoxicity in H9c2 cells was investigated, and it was found that NAC induced H9c2 cell apoptosis through the intrinsic mitochondrial pathway but not via endoplasm reticulum stress. This is, to the best of our knowledge, the first demonstration of GSH repletion-induced apoptosis via the mitochondrial pathway.

Materials and methods

Reagents and antibodies. NAC, *N*-ethylmaleimide (NEM, cat. no. E3876) and trichloroacetic acid (cat. no. T0699) were obtained from Sigma-Aldrich; Merck KGaA (Darmstadt, Germany). Tunicamycin (cat. no. T7765) was dissolved in dimethyl sulfoxide (DMSO; Sigma-Aldrich; Merck KGaA) as a 1 mg/ml stock solution and stored at -20˚C. AlamarBlue® (cat. no. DAL1025) was from Invitrogen; Thermo Fisher Scientific, Inc. (Waltham, MA, USA). Rabbit antibodies against cleaved caspase-9 (Asp353, cat. no. 9507), cleaved caspase-3 (Asp175, cat. no. 9661), cytochrome *c* (cat. no. 4272), B-cell lymphoma 2 (Bcl-2)-associated X protein (Bax, cat. no. 2772), binding immunoglobulin protein (BiP, cat. no. 3183) and C/EBP homologous protein (CHOP; cat. no. 2895) were purchased from Cell Signaling Technology, Inc. (Danvers, MA, USA).

Cell culture and cell viability. The H9c2 cell line was obtained from American Type Culture Collection (cat. no. CRL-1446; ATCC, Manassas, VA, USA). The H9c2 cells were grown in DMEM (Invitrogen; Thermo Fisher Scientific, Inc.) supplemented with 10% fetal calf serum (FCS; Invitrogen; Thermo Fisher Scientific, Inc.), 100 U/ml penicillin and 100 μg/ml streptomycin in a 5% CO_2 humidified atmosphere at 37˚C. Cell viability was determined using non-toxic alamarBlue®. The subconfluent, exponentially growing H9c2 cells at a density of $1x10^5$/ml and 100 μl medium per well were incubated with NAC for 6, 12 and 24 h. A 1/10th volume of alamarBlue® reagent was added directly to the cells in the culture medium 2 h prior to reading fluorescence (excitation at 540±35 nm and emission at 600±40 nm) using an Flx800 plate reader (BioTek Instruments, Inc., Winooski, VT, USA).

Measurement of lactate dehydrogenase (LDH) activity. The LDH activity was measured using a kit from Cayman Chemical Co. (Ann Arbor, MI, USA), which used a coupled two-step reaction. In the first step, LDH catalyzes the reduction of NAD^+ to NADH and H^+ by the oxidation of lactate to pyruvate. In the second step of the reaction, diaphorase uses the newly-formed NADH and H^+ to catalyze the reduction of a tetrazolium salt to highly-colored formazan, which absorbs at 490-520 nm. Following treatment, culture medium was collected to measure LDH activity. All the determinations were normalized to protein content, determined using the method of Lowry *et al* (13). The absorbance was recorded at 405 nm using a plate reader every 5 min for 30 min.

Immunofluorescence microscopy. The H9c2 cells at a density of $2x10^5$/well were grown on a coverslip in six-well plates for 24 h and treated with NAC and H_2O_2 for the indicated durations. The cells were then stained using Hoechst 33342 and propidium iodide (PI), which is permeant stains only dead cells. The staining pattern resulting from the simultaneous use of these dyes makes it possible to distinguish normal and dead cell populations using fluorescence microscopy.

Annexin V/PI double-staining analysis of apoptosis. Cell apoptosis was determined using Annexin V-FITC and PI double staining (Kaiji Biotechnology, Nanjing, China) according to the manufacturer's instructions. The H9c2 cells were seeded in six-well plates at a density of $1x10^5$/well and treated with different concentrations of NAC for 24 h. Following treatment, the H9c2 cells were harvested with 0.25% trypsin and washed twice in ice-cold PBS, following which they were resuspended in 300 μl of binding buffer containing 1 μg/ml PI and 0.05 μg/ml Annexin V-FITC. The samples were incubated for 15 min at room temperature in the dark and were analyzed using flow cytometry (Beckman Coulter, Inc., Miami, FL, USA) at an excitation wavelength of 488 nm. The emissions of annexin-V and PI were monitored at wavelengths of 525 and 630 nm, respectively. The percentage of apoptotic cells was determined using Multicycle software version 2.5 (Phoenix Flow Systems, San Diego, CA, USA).

Analysis of the activities of caspase-3, -8, -9 and -12. Caspase activity within the treated cells was determined fluorometrically using a Caspase-3 Fluorescence Assay kit (cat. no. 10009135; Cayman Chemical Co.), Caspase-8 Fluorescence Assay kit (cat. no. K112; BioVision, Inc., Milpitas, CA, USA), Caspase-9 Fluorescence Assay kit (cat. no. K118; BioVision, Inc.) and Caspase-12 Fluorescence Assay kit (cat. no. K139; BioVision, Inc.). These assays are based on detecting the cleavage of substrates N-Ac-DEVD-N'-MC-R110, IETD-AFC, LEHD-AFC and ATAD-AFC. The treated cells ($5x10^5$) were pelleted and resuspended in 50 μl of chilled cell lysis buffer, and transferred to a 96-well plate. Caspase buffer (50 μl) containing 50 μM substrate was added to the sample and cleavage of substrate was performed at 37˚C using an Flx800 plate reader (BioTek Instruments, Inc.).

Subcellular fractionation, SDS-PAGE and immunoblotting. The whole cell lysate was extracted using 1X SDS buffer. The cytosolic and mitochondrial fractions were prepared using a Mitochondria/Cytosol Isolation kit (Abcam, Cambridge, UK). The protein contents of the subcellular fractions and whole cell lysate were determined by BCA protein assay kit and 30 μg of samples were separated on a 12% glycine SDS-PAGE gel and transferred onto a PVDF membrane. The membranes were blocked in 5% dry milk in TBS with 0.1% Tween-20 (TBST) for 1 h at room temperature, followed by incubation with the indicated primary antibodies to cytochrome *c* (1:1,000), Bax (1:1,000), GAPDH (1:2,000), VDAC (1:1,000), BiP (1:1,000) and CHOP (1:1,000) and subsequent incubation with horseradish peroxidase goat anti-rabbit IgG secondary antibody (cat. no. 7074, 1:10,000; Cell Signaling Technology,

Inc.) in TBST with 0.2% BSA for 1 h at room temperature. The immunoblot signals were visualized using Super Signal West Pico Chemiluminescent substrate (Pierce; Thermo Fisher Scientific, Inc.).

NEM-alkylated redox western blot analysis. For protein disulfide isomerase (PDI) redox analysis, the cells were treated with NAC or 10 mM DTT for the indicated time and washed twice with ice-cold PBS immediately following treatment. The cells were then precipitated with chilled trichloroacetic acid (10%) for 30 min at 4˚C. The samples were centrifuged at 12,000 x g for 10 min at room temperature and washed twice with 100% acetone. The protein pellets were dissolved in non-reducing buffer containing 100 mM Tris-HCl (pH 6.8), 2% SDS and 40 mM NEM. PDI redox forms were separated via 10% non-reducing SDS-PAGE.

Measurement of changes in mitochondrial membrane potential ($\Delta\psi m$). Mitochondrial transmembrane depolarization was detected using JC-1 (Molecular Probes; Thermo Fisher Scientific, Inc.). Following washing twice with pre-warmed PBS, 2 μg/ml JC-1 was added into each well and incubated at 37˚C for 30 min. The cells were then washed three times with pre-warmed PBS. NAC (4 μM) was added and the cell culture plate was incubated at 37˚C for the required duration. The plates were immediately read using the Flx800 plate reader (BioTek Instruments, Inc.). Red fluorescence was measured at 550 nm (excitation) and 600 nm (emission). Green fluorescence was measured at 485 nm (excitation) and 535 nm (emission). The ratio of red fluorescence to green fluorescence was determined, and mitochondrial depolarization was indicated by a decrease in the red/green fluorescence ratio.

Reverse transcription-quantitative polymerase chain reaction (RT-qPCR) analysis. The untreated and treated H9c2 cells were rinsed twice with PBS. The total RNA was extracted using TRIzol reagent (Invitrogen; Thermo Fisher Scientific, Inc.). cDNA was synthesized from 1 μg total RNA using reverse transcription reagents from Applied Biosystems; Thermo Fisher Scientific, Inc., according to the manufacturer's instructions. PCR amplifications were performed using 10 μl SYBR-Green PCR Master mix, 2 μl cDNA sample (equivalent to 100 ng) and 1 μl of 2 μM forward and reverse primers on the ABI Prism 7000 Sequence Detection system (Applied Biosystems; Thermo Fisher Scientific, Inc.) according to the following thermal cycling conditions: 95˚C for 10 min, 40 cycles of 95˚C for 15 sec and 60˚C for 30 sec. PCR amplifications were performed in duplicate wells. The quantification was performed using the comparative quantification cycle ($2^{-\Delta\Delta Cq}$) method (14), using human GAPDH as an internal control.

Statistical analysis. All experiments were repeated three times. For the western blot analysis, one representative image is shown in figures. SPSS software version 22.0 (IBM Corp., Armonk, NY, USA) was used for statistical analysis. Values are presented as the mean ± standard deviation. Student's t-test was used for statistical analysis. $P<0.05$ was considered to indicate a statistically significant difference.

Results

NAC induces the apoptosis of H9c2 cells. Firstly, the present study investigated the effects of NAC treatment on the growth of H9c2 cells by using the alamarBlue® assay. Compared with the control group, the viability of H9c2 cells was significantly decreased in a dose-dependent manner in response to 1, 2 and 4 μM of NAC for 24 h (Fig. 1A). LDH release was also measured in the supernatant of the NAC-treated H9c2 cells. NAC treatment induced the release of LDH in a dose- and time-dependent manner (Fig. 1B).

To determine whether the observed decrease in cell viability was associated with apoptosis or necrosis, the nuclear morphology and plasma membrane permeability of the NAC-treated H9c2 cells were examined using Hoechst 33342 (blue) and PI (red) staining. In the H_2O_2-treated cells, the rate of necrosis was markedly increased, whereas treatment with 2 or 4 μM NAC had effect on the rate of necrosis (Fig. 1C). The ability of NAC to induce H9c2 cell apoptosis was quantified using Annexin V-FITC/PI double staining and was calculated using Multicycle software. Following treatment with various concentrations of NAC for 24 h, the percentages of apoptotic cells were 18.6±4.1 and 24.5±3.7%, respectively, which was significantly higher, compared with that in the untreated control cells (5.4±1.8, $P<0.01$; Fig. 1D).

Activation of caspase-9 and -3, but not caspase-8, is involved in NAC-induced apoptosis of H9c2 cells. The present study also investigated the possible mechanisms underlying the NAC-induced apoptosis of H9c2 cells. As caspases are known to be pivotal in mediating various apoptotic signals, the present study measured the activity of initiator caspases (caspase-8 and -9) and effector caspase (caspase-3) in the NAC-treated H9c2 cells using fluorometrical assay kits. As shown in Fig. 2, exposure of the H9c2 cells to 4 μM of NAC led to increased enzymatic activities of caspase-3 and -9 in a time-dependent manner during the treatment period (Fig. 2A and B). The increased activities of caspases-3 and -9 were observed as early as 12 h. By contrast, no significant change in the activity of caspase-8 was observed (Fig. 2C). The NAC-induced caspase activation was further confirmed by detecting the cleavage of procaspase-9 and procaspase-3 following NAC treatment in H9c2 cells (Fig. 2D).

NAC induces apoptosis through activation of the intrinsic mitochondrial signaling pathway in H9c2 cells. Apoptosis is usually induced via two main pathways involving either the activation of death receptors (extrinsic pathway) or the mitochondrial pathway (intrinsic pathway). The death receptor pathway is usually triggered by the binding of death receptors, including Fas or tumor necrosis factor receptor, by their respective ligands, namely FasL and TNFRL, which recruit initiator caspase-8 via the adaptor protein, FADD, leading to the proteolytic activation of caspase-8 (15). Consistent with the results of caspase-8 activity, NAC treatment did not affect the levels of Fas or FasL (Fig. 3A). These results suggested that NAC treatment did not activate the Fas-mediated death receptor pathway in H9c2 cells.

Mitochondria are key in the regulation of apoptosis. One of the major events in mitochondrial dysfunction is the loss

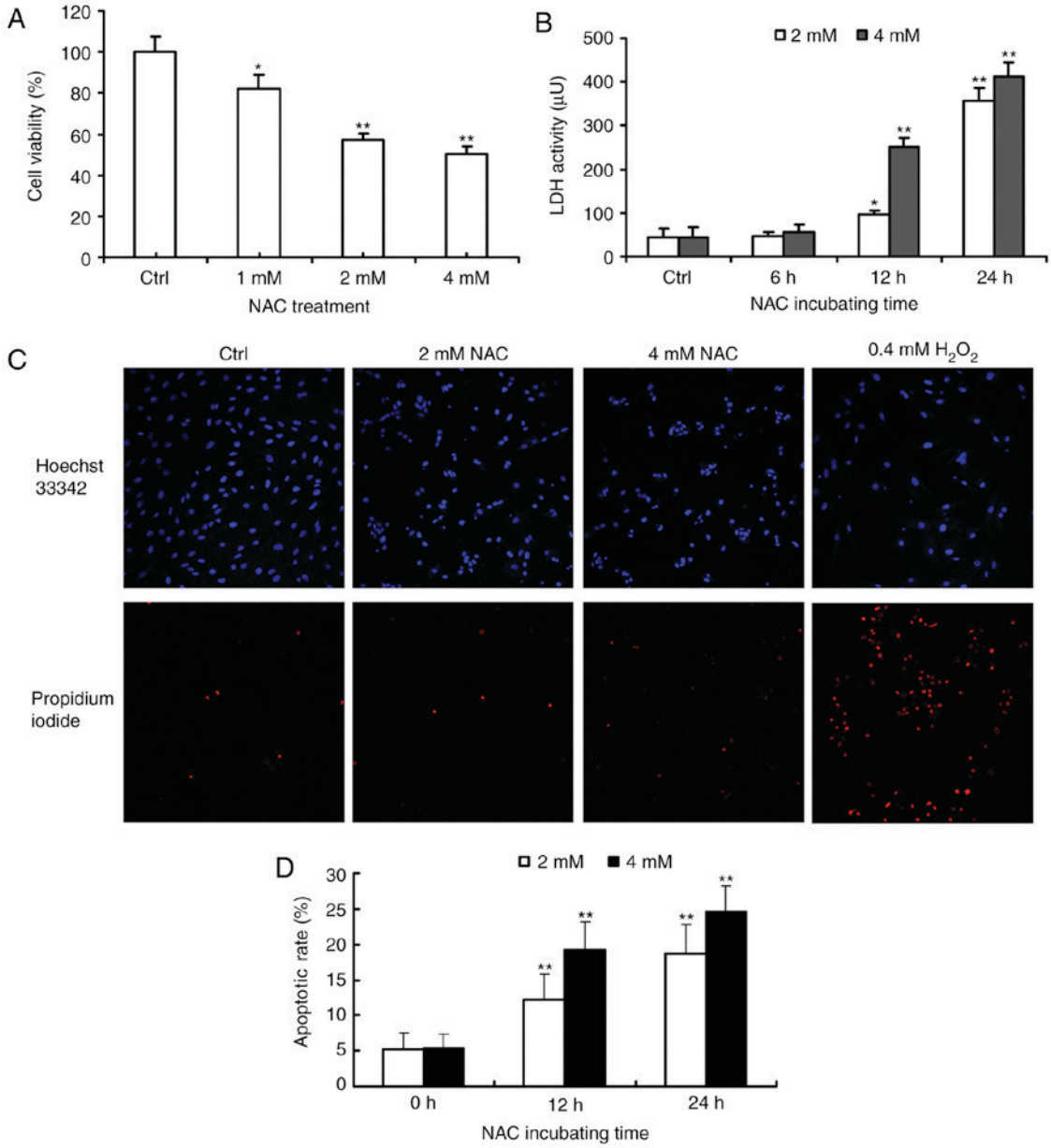

Figure 1. NAC induces concentration- and time-dependent apoptosis in H9c2 cells. (A) Cell viabilities were determined using an alamarBlue® assay. The values were calculated relative to the control group. (B) LDH activity was measured in the supernatant of NAC-treated H9c2 cells. The results are presented as the mean ± standard deviation and are representative of three independent experiments. (C) Cells were treated with NAC and H_2O_2 for 24 h. The nuclear morphology of H9c2 cells was observed under a fluorescent microscope following Hoechst 33342 and propidium iodide staining (magnification, x400). (D) NAC-treated cells were stained with Annexin V-FITC and propidium iodide followed by flow cytometric analysis. The Annexin V-positive cells were regarded as apoptotic. Values are presented as the mean ± standard deviation (n=3). *P<0.05 and **P<0.01 vs. Ctrl group. NAC, *N*-acetylcysteine; Ctrl, control; LDH, lactate dehydrogenase.

of Δψm and the subsequent release of cytochrome *c* (16). The present study investigated Δψm using the dual-emission fluorescent dye, JC-1, which characterizes the dissipation of Δψm by a significant shift of red to green fluorescence. The treatment of cells with NAC enhanced the level of green fluorescence in a time-dependent manner, which demonstrated the loss of Δψm during NAC-induced apoptosis (Fig. 3B).

The release of cytochrome *c* from mitochondria combines with apoptotic protease activating factor 1 and procaspase-9 to form the apoptosome, which leads to the activation of caspse-9 and -3. The Bcl-2 family members are known to be critical in regulating the release of cytochrome *c*. Under apoptotic stimuli, pro-apoptotic Bcl-2 members, including Bax and BH3 interacting-domain death agonist, are activated, whereas anti-apoptotic Bcl-2 and Bcl-extra large prevent this process (17). The balance of pro- and anti-apoptotic proteins is associated with the ultimate fate of cells. To assess whether the mitochondrial pathway was involved in NAC-induced apoptosis, the present study detected the levels of cytochrome *c* and Bax in proteins extracts from cytosolic and mitochondrial fractions of the NAC-treated cells. The release of cytochrome *c* from the mitochondria to the cytosol was observed as early as 2 h following treatment (Fig. 3C). Consistent with this, a time-dependent increase in mitochondrial Bax and a concomitant decrease in the cytosolic fraction were observed (Fig. 3C). The expression levels of Bax and

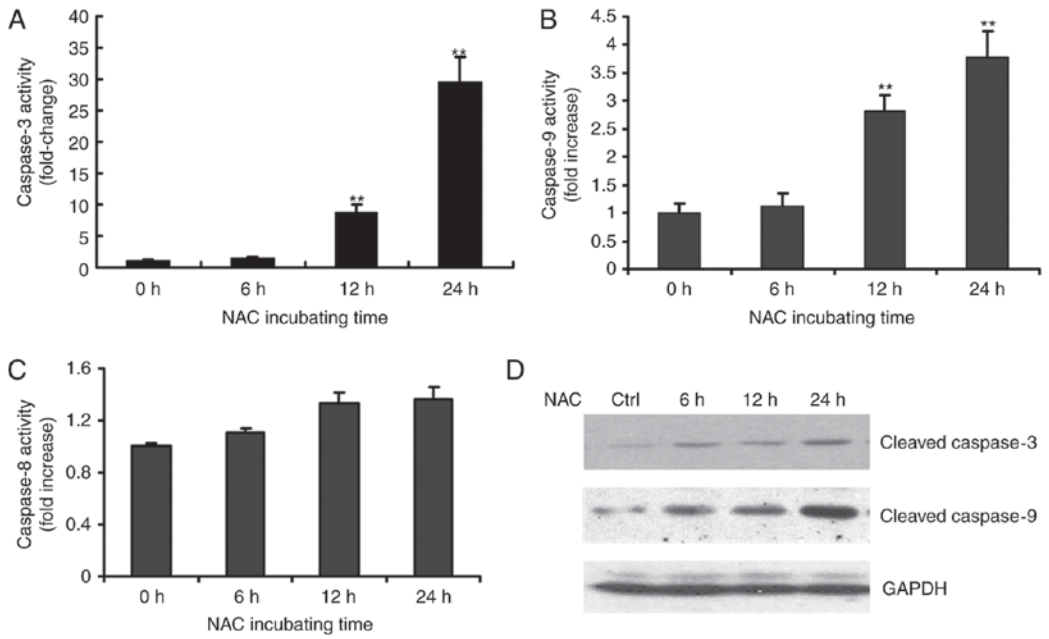

Figure 2. NAC-induced apoptosis is mediated by the activation of caspase-9 and -3 in H9c2 cells. H9c2 cells were incubated with 4 μM NAC for indicated durations. The enzymatic activities of (A) caspase-3, (B) caspase-9 and (C) caspase-8 were measured using fluorescence assay kits. The results are presented as the mean ± standard deviation and are representative of three independent experiments. **P<0.01 vs. Ctrl group. (D) Whole cell lysates were subjected to western blot analysis to detect cleavage of procaspase-3 and -9 using cleaved procaspase-9 and -3 antibodies. The data shown are representative of three independent experiments. NAC, *N*-acetylcysteine; Ctrl, control.

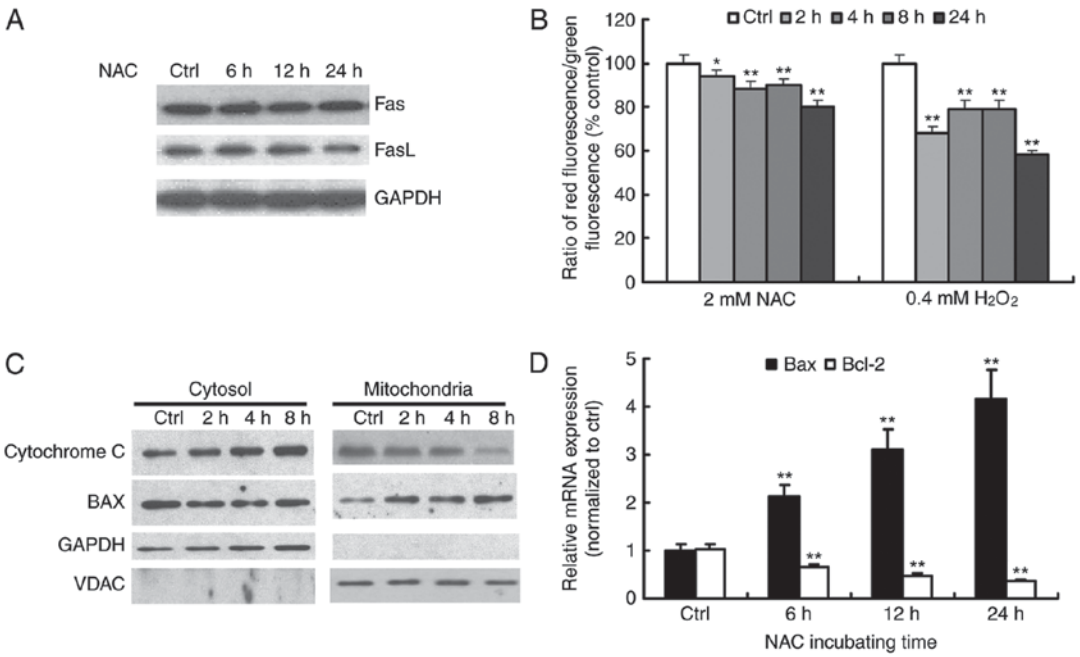

Figure 3. NAC induces apoptosis through activation of the intrinsic mitochondrial signaling pathway in H9c2 cells. (A) Whole cell lysates were subjected to western blot analysis to detect Fas and FasL. Equal loading was confirmed by reprobing the blots with an antibody against GAPDH. The data shown are representative of three independent experiments. (B) Mitochondrial membrane potential was detected using JC-1 on an Flx800 plate reader. The results are presented as the mean ± standard deviation and are representative of three independent experiments. *P<0.05 and **P<0.01 vs. Ctrl group. (C) Levels of cytochrome *c* and Bax were measured in the cytosolic and mitochondrial fractions using western blot analysis. VDAC and GAPDH were used as internal controls for the mitochondrial and the cytosolic fractions, respectively. All data shown are representative of three independent experiments. (D) mRNA expression levels of BAX and Bcl-2 were detected using reverse transcription-quantitative polymerase chain reaction analysis. Values are presented as the mean ± standard deviation (n=3). **P<0.01 vs. Ctrl group. NAC, *N*-acetylcysteine; Ctrl, control; FasL, Fas ligand; Bcl-2, B-cell lymphoma 2; Bax, Bcl-2-associated X protein.

Bcl-2 were examined using RT-qPCR analysis. As shown in Fig. 3D, following exposure of the H9c2 cells to 4 μM NAC for different durations (0-24 h), The mRNA levels of Bax increased, whereas the mRNA levels of Bcl-2 decreased gradually with time. Therefore, NAC treatment increased the ratio of Bax/Bcl-2, which favors the occurrence of apoptosis.

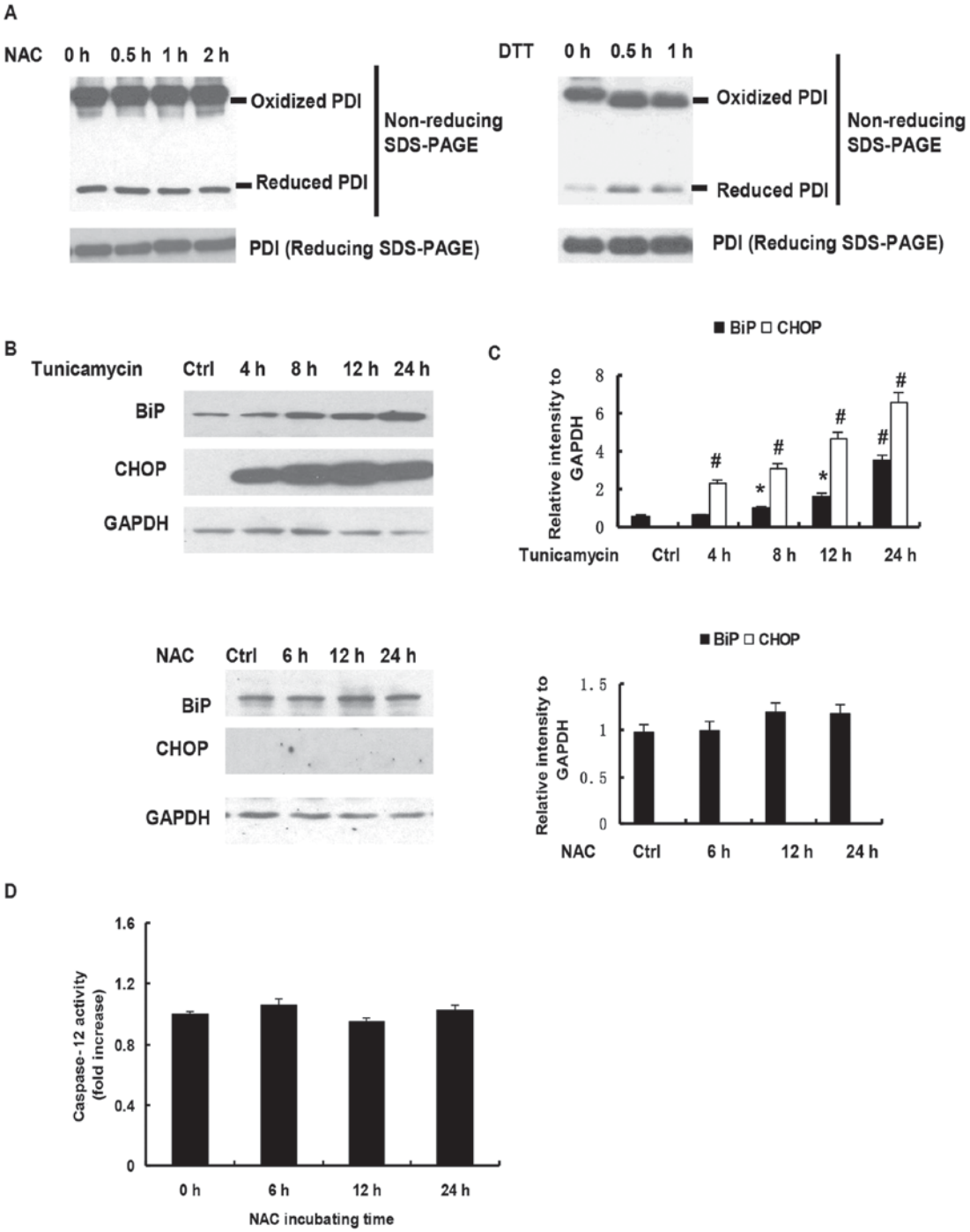

Figure 4. NAC treatment does not induce ER stress. (A) Redox western blot analysis was performed to investigate the redox state of PDI following NAC or DTT treatment. For reducing SDS-PAGE, 5% DTT was added to the samples. (B) Whole cell lysates were subjected to western blot analysis to detect BiP and CHOP following NAC or tunicamycin treatment. Equal loading was confirmed by reprobing of the blots with an antibody against GAPDH. All data shown are representative of three independent experiments. (C) Densitometry values of BiP and CHOP after NAC or tunicamycin treatment are represented as relative intensities to GAPDH in mean arbitrary units using ImageJ software version 1.50i. The levels were averaged over three experiments and plotted. *P<0.05 or $^{\#}$P<0.001 vs. Ctrl. (D) H9c2 cells were incubated with 4 μM NAC for the indicated durations. The enzymatic activities of caspase-12 were measured using fluorescence assay kits. The results are presented as the mean ± standard deviation and are representative of three independent experiments. NAC, *N*-acetylcysteine; Ctrl, control; DTT, dithiothreitol; PDI, protein disulfide isomerase; BiP, binding immunoglobulin protein; CHOP, C/EBP homologous protein.

These results suggested that NAC-induced apoptosis occurred mainly through the mitochondria-dependent pathway.

NAC induced apoptosis is independent of ER stress. In the ER, nascent proteins are folded with the assistance of ER chaperones. The highly oxidized redox milieu of the ER matrix facilitates disulfide bond formation and the maturation of secretory proteins. Exogenous reductants disrupt disulfide bond formation and abrogate oxidative protein folding in the ER, which triggers the ER stress response. Our previous study demonstrated that the repletion of GSH by NAC in H9c2 cells caused a reduction of the glutathione redox potential. To

examine whether NAC exposure induced H9c2 cell apoptosis through altering the oxidized environment in ER and causing ER stress, the present study analyzed the redox state of PDI. PDI is an essential chaperone, which constitutes 2% of the protein in the ER and has long been known to assist in the formation of disulfide bonds. PDI is found predominantly in an oxidized form *in vivo* (18). As shown in Fig. 4A, NEM derivatization allowed the identification of reduced PDI and oxidized PDI, which migrates at a slower rate than the reduced form. Following reduction with DTT, PDI shifted to the reduced isoform, whereas minimal change in reduced PDI was observed on exposure to NAC for 2 h (Fig. 4A). Further analysis showed that the levels of BiP and CHOP were significantly upregulated in the H9c2 cells treated with tunicamycin, a common agent to induce ER stress, but not in NAC-treated H9c2 cells (Fig. 4B and C). Increasing evidence has demonstrated that caspase-12 is key in ER stress-mediated apoptosis (19). In the present study, no change in caspase-12 activity was observed following NAC treatment (Fig. 4D). Taken together, these data indicated that exogenous GSH repletion by NAC-induced H9C2 cell apoptosis was independent of ER stress in H9c2 cells.

Discussion

As an antioxidant precursor to glutathione, the clinical applications of NAC have broadened. NAC appears to be promising in the treatment of several illnesses, including chronic obstructive pulmonary disease and contrast-induced nephropathy (20). There is also evidence to support its use in Alzheimer's disease and psychiatric disorders, particularly schizophrenia and bipolar disorder (21). The primary mechanisms underlying the beneficial effects for these disorders may be that NAC maintains the redox balance in the cell through augmentation of intracellular glutathione levels and its scavenging activity of free radicals (22). NAC is safe and well tolerated when administered orally, but has documented risks on intravenous administration.

Although NAC can inhibit H_2O_2-mediated cell death, it enhances the apoptosis induced by other stimuli, including hypoxia, ultraviolet, imatinib, 5-fluorouracil and fisetin. NAC can also induce apoptosis in specific cells. Tsai *et al* (23) reported that NAC induces apoptosis in rat and human smooth muscle cells, and that the overexpression of Bcl-2 suppressed the cell death induced by NAC. Consistent with these results, the present study showed that NAC was cytotoxic towards H9c2 cells through inducing apoptosis. The increased apoptosis was not attributable to the extrinsic apoptosis pathway due to the lack of activation of caspase-8, and no increase in the levels of Fas and FasL in response to NAC. By contrast, NAC appeared to increase the activities of caspase-9 and -3, and the cleavage of procaspase-9 and -3. Bcl-2 family proteins are known to be either pro-apoptotic or anti-apoptotic via regulating the permeability of the mitochondrial outer membrane. Bcl-2 is anti-apoptotic and the Bax protein is pro-apoptotic in initiating apoptosis. The data obtained in the present study showed that NAC resulted in the simultaneous upregulation of Bax and downregulation of Bcl-2, loss of $\Delta\psi m$, and the subsequent release of cytochrome *c* and translocation of Bax to mitochondria. These results support the hypothesis that NAC-induced apoptosis in H9c2 cells is mediated by the intrinsic mitochondrial pathway.

The mitochondrion is the most important organelle in determining continued cell survival and cell death. GSH/GSSG ratios of 20:1-40:1 and reduced milieu have been reported in the matrix of mitochondria, whereas its inner membrane space is more oxidizing (1). Our previous investigations (12) revealed that the repletion of GSH from NAC in H9c2 cells disrupted the reduced milieu of mitochondria, which was confirmed by the redox states of mitochondrial thrioredoxin 2 and roGFP. A previous study also showed that GSH ethyl ester or NAC induce mitochondrial oxidation via respiratory complex III (24). Singh *et al* (25) reported that NAC reductive stress impairs L6 myoblast mitochondrial respiratory chain function, leading to mitochondrial ROS production and the activation of mitochondrial biogenesis pathways. These findings further clarify the possible mechanism by which the mitochondria pathway is involved in NAC-induced apoptosis.

GSH is known to be present in the ER, and the redox status of the ER is defined by the status of glutathione. This compartment contains millimolar concentrations of GSH and GSSG, in which the GSH/GSSG ratio ranges between 1:1 and 3:1 to achieve a more oxidizing environment (26). Previous findings have demonstrated that BiP and CHOP are upregulated in HeLa cells following treatment with NAC, and that the protein kinase R-like ER kinase-activating transcription factor 4 pathway is activated in NAC-treated cells, indicating that NAC-induced apoptosis in HeLa cells is mediated by the ER stress pathway (27). By contrast, the present study found that NAC did not upregulate the expression of BiP or CHOP in H9c2 cells. The fact that the redox status of PDI did not alter following exposure to NAC was consistent with NAC causing a decreased GSH/GSSG ratio due to a corresponding increase in GSSG. This observation suggests that the mechanism of NAC-induced apoptosis in H9c2 cells and HeLa cells is cell type-specific.

To the best of our knowledge, the present study is the first to show that NAC induced the apoptosis of H9c2 cells via the mitochondria-dependent pathway but not via ER stress, and that exogenous GSH from NAC did not alter the oxidized milieu of the ER.

Acknowledgements

This study was supported by the National Natural Science Foundation of China (grant nos. 81270279 and 81471897) and the Hunan Natural Science Foundation (grant no. 2013JJ1009).

References

1. Hansen JM, Go YM and Jones DP: Nuclear and mitochondrial compartmentation of oxidative stress and redox signaling. Annu Rev Pharmacol Toxicol 46: 215-234, 2006.
2. Harris C and Hansen JM: Oxidative stress, thiols and redox profiles. Methods Mol Biol 889: 325-346, 2012.
3. Schafer FQ and Buettner GR: Redox environment of the cell as viewed through the redox state of the glutathione disulfide/glutathione couple. Free Radic Biol Med 30: 1191-1212, 2001.
4. Trotter EW and Grant CM: Thioredoxins are required for protection against a reductive stress in the yeast Saccharomyces cerevisiae. Mol Microbiol 46: 869-878, 2002.
5. Rajasekaran NS, Connell P, Christians ES, Yan LJ, Taylor RP, Orosz A, Zhang XQ, Stevenson TJ, Peshock RM, Leopold JA, *et al*: Human alpha B-crystallin mutation causes oxido-reductive stress and protein aggregation cardiomyopathy in mice. Cell 130: 427-439, 2007.

6. Rand JD and Grant CM: The thioredoxin system protects ribosomes against stress-induced aggregation. Mol Biol Cell 17: 387-401, 2006.
7. Mayer M and Noble M: *N*-acetyl-L-cysteine is a pluripotent protector against cell death and enhancer of trophic factor-mediated cell survival in vitro. Proc Natl Acad Sci USA 91: 7496-7500, 1994.
8. Park SA, Choi KS, Bang JH, Huh K and Kim SU: Cisplatin-induced apoptotic cell death in mouse hybrid neurons is blocked by antioxidants through suppression of cisplatin-mediated accumulation of p53 but not of Fas/Fas ligand. J Neurochem 75: 946-953, 2000.
9. Rakshit S, Bagchi J, Mandal L, Paul K, Ganguly D, Bhattacharjee S, Ghosh M, Biswas N, Chaudhuri U and Bandyopadhyay S: *N*-acetyl cysteine enhances imatinib-induced apoptosis of Bcr-Abl$^+$ cells by endothelial nitric oxide synthase-mediated production of nitric oxide. Apoptosis 14: 298-308, 2009.
10. Wu MS, Lien GS, Shen SC, Yang LY and Chen YC: *N*-acetyl-L-cysteine enhances fisetin-induced cytotoxicity via induction of ROS-independent apoptosis in human colonic cancer cells. Mol Carcinog 53 (Suppl 1): E119-E129, 2014.
11. Qanungo S, Wang M and Nieminen AL: *N*-Acetyl-L-cysteine enhances apoptosis through inhibition of nuclear factor-kappaB in hypoxic murine embryonic fibroblasts. J Biol Chem 279: 50455-50464, 2004.
12. Zhang H, Limphong P, Pieper J, Liu Q, Rodesch CK, Christians E and Benjamin IJ: Glutathione-dependent reductive stress triggers mitochondrial oxidation and cytotoxicity. FASEB 26: 1442-1451, 2012.
13. Lowry OH, Rosebrough NJ, Farr AL and Randall RJ: Protein measurement with the Folin phenol reagent. J Biol Chem 193: 265-275, 1951.
14. Livak KJ and Schmittgen TD: Analysis of relative gene expression data using real-time quantitative PCR and the 2(-Delta Delta C(T)) method. Methods 25: 402-408, 2001.
15. Elmore S: Apoptosis: A review of programmed cell death. Toxicol Pathol 35: 495-516, 2007.
16. Kuznetsov AV, Margreiter R, Amberger A, Saks V and Grimm M: Changes in mitochondrial redox state, membrane potential and calcium precede mitochondrial dysfunction in doxorubicin-induced cell death. Biochim Biophys Acta 1813: 1144-1152, 2011.
17. Sharpe JC, Arnoult D and Youle RJ: Control of mitochondrial permeability by Bcl-2 family members. Biochim Biophys Acta 1644: 107-113, 2004.
18. Mezghrani A, Fassio A, Benham A, Simmen T, Braakman I and Sitia R: Manipulation of oxidative protein folding and PDI redox state in mammalian cells. EMBO J 20: 6288-6296, 2001.
19. Morishima N, Nakanishi K, Takenouchi H, Shibata T and Yasuhiko Y: An endoplasmic reticulum stress-specific caspase cascade in apoptosis. Cytochrome *c*-independent activation of caspase-9 by caspase-12. J Biol Chem 277: 34287-34294, 2002.
20. Dodd S, Dean O, Copolov DL, Malhi GS and Berk M: *N*-acetylcysteine for antioxidant therapy: Pharmacology and clinical utility. Expert Opin Biol Ther 8: 1955-1962, 2008.
21. Dean O, Giorlando F and Berk M: *N*-acetylcysteine in psychiatry: Current therapeutic evidence and potential mechanisms of action. J Psychiatry Neurosci 36: 78-86, 2011.
22. Aruoma OI, Halliwell B, Hoey BM and Butler J: The antioxidant action of *N*-acetylcysteine: Its reaction with hydrogen peroxide, hydroxyl radical, superoxide, and hypochlorous acid. Free Radic Biol Med 6: 593-597, 1989.
23. Tsai JC, Jain M, Hsieh CM, Lee WS, Yoshizumi M, Patterson C, Perrella MA, Cooke C, Wang H, Haber E, *et al*: Induction of apoptosis by pyrrolidinedithiocarbamate and *N*-acetylcysteine in vascular smooth muscle cells. J Biol Chem 271: 3667-3670, 1996.
24. Kolossov VL, Beaudoin JN, Ponnuraj N, DiLiberto SJ, Hanafin WP, Kenis PJ and Gaskins HR: Thiol-based antioxidants elicit mitochondrial oxidation via respiratory complex III. Am J Physiol Cell Physiol 309: C81-C91, 2015.
25. Singh F, Charles AL, Schlagowski AI, Bouitbir J, Bonifacio A, Piquard F, Krähenbühl S, Geny B and Zoll J: Reductive stress impairs myoblasts mitochondrial function and triggers mitochondrial hormesis. Biochim Biophys Acta 1853: 1574-1585, 2015.
26. Hwang C, Sinskey AJ and Lodish HF: Oxidized redox state of glutathione in the endoplasmic reticulum. Science 257: 1496-1502, 1992.
27. Guan D, Xu Y, Yang M, Wang H, Wang X and Shen Z: *N*-acetyl cysteine and penicillamine induce apoptosis via the ER stress response-signaling pathway. Mol Carcinog 49: 68-74, 2010.